ORIGINAL CONTRIBUTION

Linear and nonlinear shear rheology of nearly unentangled H-polymer melts and solutions

Vincenzo Ianniello[1] · Salvatore Costanzo[1]

Abstract

We investigate the linear and nonlinear shear rheology of a marginally entangled H-polymer melt and two solutions made by diluting high molecular weight H-polymers in linear oligomer. In order to approach a nearly unentangled state, dilution is conducted at volume fractions such that the two solutions attain a similar number of entanglements of the melt. Start-up shear experiments demonstrate that the nonlinear behavior of the H-polymer melt is analogous to that of a linear melt with comparable span chain length. Concerning solutions, the increase of chain elasticity in fast flows, coupled with a lesser role of monomeric friction reduction, allows to attain strong stretch in start-up shear tests. As a result, transient strain hardening occurs. Furthermore, a failure of the Cox-Merz rule is observed for the solutions, which indicates that they better conform to a FENE-Rouse chain behavior compared to melts.

Keywords H-polymers · Shear hardening · Cone-and-partitioned plate · Nonlinear rheology

Introduction

Decoding molecular dynamics of polymers with complex topology is a crucial objective for both polymer science and industrial applications. It promotes the development of new ideas for refining molecular models and provides new strategies for tailoring the flow properties of materials. Among complex architectures, branched polymers represent the largest category, ranging from simple structures such as 3-arm stars to intricate macromolecules such as dendronized polymers.

Dynamics of entangled branched polymers can be rationalized on the basis of the tube model Doi and Edwards 1978a, b, c, 1979; de Gennes 1971; Likhtman et al. 2000; Milner et al. 2001; Graham et al. 2003 with the addition of new physics accounting for the ramified architecture. The new ideas embedded in tube-based algorithms for branched systems included arm breathing, additional friction arising

from the branch points, hierarchical relaxation and dynamic tube dilation McLeish 1988; Park et al. 2005; Karayiannis and Mavrantzas 2005; Nielsen et al. 2006; Ianniruberto and Marrucci 2013; Watanabe 2008; Narimissa et al. 2016. The relaxation of a branched polymer starts from the free ends of the outer branches and proceeds inward in a hierarchical fashion. Friction is mainly concentrated at the branching points, whose diffusion is much slower than arm breathing dynamics. On the other hand, relaxed branches can act as an effective solvent for the unrelaxed inner portions of the molecules, enlarging the tube and eventually accelerating relaxation dynamics. The idea of dynamic tube dilation (DTD) was first proposed in the seminal work of Marrucci (1985) for entangled binary blends of linear chains. It was postulated that the constraint release (CR) effect of the short chains induces an enlargement of the initial tube in which a long chain is confined. The tube diameter $a(t)$ increases with time as $a(t) = a_0[\phi(t)]^{-\alpha/2}$, where a_0 is the initial tube diameter, $\phi(t)$ is the dilation factor given by the effective fraction of initial constraints surviving at time t, and α is the dilution exponent van Ruymbeke et al. 2014. The latter can vary between 1 and 4/3. The relaxation function, $\mu(t) = G(t)/G_N^0$, can then be written as $\mu(t) = \varphi'[\phi(t)]^{\alpha}$, where φ' is the unrelaxed fraction of the initial tube segments Lentzakis et al. 2019. If the CR motion of the long chain is fast enough to fully explore, at time t, the dilated tube, then the relaxed

✉ Salvatore Costanzo
  salvatore.costanzo@unina.it

  Vincenzo Ianniello
  vincenzo.ianniello@unina.it

1 Department of Chemical, Materials and Production Engineering, University of Naples Federico II, P.le Tecchio 80, Naples 80125, Italy

chains act as an effective solvent and the relaxation function assumes the simple form $\mu(t) = [\varphi'(t)]^{1+\alpha}$. If CR motion is slow, then the diameter of the effective tube explored by the chain is smaller than $a(t)$. The latter scenario is defined as partial DTD. By combining viscoelastic and dielectric data, it was found that partial DTD could provide a more general picture for the relaxation of linear polymer blends Watanabe et al. 2004; Matsumiya et al. 2013 and could be invoked to explain the rheological properties of star, Cayley-tree, and H-polymers Watanabe et al. 2006, 2008; Matsumiya et al. 2014; Lentzakis et al. 2019. Extensions of the tube model with the ingredients above were successfully implemented for stars Doi and Kuzuu 1980; Pearson and Helfand 1984; Dubbeldam and Molenaar 2009, pompom polymers McLeish 1988; McLeish et al. 1999; Ianniruberto and Marrucci 2013, combs Snijkers et al. 2013 and more complex branched architectures Das et al. 2006; van Ruymbeke et al. 2010; Park et al. 2005; Wagner et al. 2000, for both linear and nonlinear flow regimes. Based on DTD picture, analogies could be drawn between pompom polymers and linear blends. In particular, it was found that the linear viscoelastic relaxation spectrum of a pompom polymer with long entangled backbone and short unentangled branches is identical to that of a blend of entangled linear chains in a short linear matrix, provided that the blend is properly designed. To this end, the molecular weight of the long linear chain must be equal to that of the span molecular weight of the pompom polymer, given by the sum of the backbone molecular weight and that of two branches. Furthermore, the volume fraction of long linear chains in the blend must be equal to the ratio between the span molecular weight and the total molecular weight of the pompom polymer van Ruymbeke et al. 2007.

Nonlinear flow behavior of branched polymers is relevant for many practical applications, particularly in transient conditions. Extensional data on long chain branched polymers demonstrated that strain hardening appears at relatively low rates and increases with the degree of branching Hatzikiriakos 2000; Stadler et al. 2009; Morelly and Alvarez 2020, a peculiarity particularly relevant for processing. The onset of extensional hardening at low rates is observed for model systems Huang et al. 2017 as well. Analogous experiments on well-defined model polymers were performed in start-up shear flow Snijkers et al. 2013a, b, c; Snijkers and Dimitris 2014; Huang et al. 2017; Costanzo et al. 2016; Scherz et al. 2017. The main outcome is that branched polymer melts are shear thinning and they exhibit a broader viscosity overshoot than linear polymers due to the broader spectrum of relaxation times. For branched architectures featuring a backbone such as comb polymers, if the relaxation time scales of the branches and the backbone are well separated, a double overshoot is observed Snijkers et al. 2013. The first overshoot reflects branches withdrawal into the backbone tube whereas the second peak is associated with backbone stretch Snijkers

et al. 2013. The latter seems to be also associated to a pronounced stress undershoot at high shear rates Snijkers et al. 2013. Star and regular dendrimers are found to verify Cox-Merz rule Cox and Merz 1958. Conversely, for branched systems such as combs, Cox-Merz rule is not always obeyed Snijkers and Dimitris 2014. Although such rule is empirical, and therefore not requested to hold always, it was speculated that the failure can be ascribed to extra stress coming from the backbone stretch. The latter occurs to a larger extent with increasing number of branches, that is, with increasing backbone dilution.

Polymer solutions made of entangled polymers diluted in oligomers were used to investigate differences between entangled linear melts and solutions in fast flows. Huang et al. demonstrated that melts and solutions with the same number of entanglements, Z, have the same reduced linear viscoelastic properties, yet the nonlinear extensional behavior is remarkably different Huang et al. 2013. Melts undergo extensional viscosity thinning whereas solutions undergo hardening. The viscosity thinning of the melts is due to anisotropic monomeric friction reduction caused by the strong alignment of the chains in the flow direction, particularly in extensional flows Matsumiya and Watanabe 2021. Friction reduction is less relevant in solutions as the long chains experience a nearly isotropic environment due to the fast relaxation of the oligomers. Therefore, the larger the molecular weight of the oligomer, the larger becomes the friction reduction effect Ianniruberto et al. 2012. Moreover, strain hardening of solutions with the same number of entanglements increases with increasing maximum chain stretch ratio Huang et al. 2015. The universality of behavior between melts and solutions can be eventually recovered by matching the same number of entanglements, the same friction reduction between melt and oligomeric solvent, and the same number of Kuhn segments between entanglements, that is, the same maximum stretch ratio Wingstrand et al. 2015. The difference observed in extensional flow could not be detected in shear due to the vorticity component of the flow Costanzo et al. 2016.

The linear and nonlinear behavior of poorly entangled polymers is less explored. Works available in literature mainly concern unentangled linear melts Santangelo and Roland 2001; Colby et al. 2007; Matsumiya et al. 2018; Watanabe et al. 2021; Sato et al. 2021, whereas systematic studies on unentangled or poorly entangled solutions of macromolecules in oligomeric solvents are lacking. As mentioned above, in entangled regime, a direct comparison between melts and solutions could be made, as Z is the only governing parameter for linear viscoelasticity. Conversely, the characteristic length to consider in comparing melts and solutions in unentangled state is not straightforward.

Concerning nonlinear behavior, unentangled melts undergo viscosity thinning in both shear and extension

Colby et al. 2007; Matsumiya et al. 2018. In particular, the power law exponent of shear thinning (-0.5) is smaller compared to entangled systems (approximately -0.9). The thinning exponent of -0.5 indicates that unentangled melts, generally modelled as Rouse chains, obey the Cox-Merz rule Colby et al. 2007. Viscosity thinning in unentangled melts arises from the competing effect of increased elasticity due to the FENE behavior of the chains Matsumiya et al. 2018 and monomeric friction reduction Ianniruberto et al. 2012. Recently, it was also remarked that Brownian force intensity may change with flow, affecting the dependence of viscosity on flow strength Matsumiya et al. 2018; Sato et al. 2021. Changes of friction reduction and Brownian force intensity are necessary ingredients for a quantitative description of the thinning behavior of viscosity and first normal stress coefficient of unentangled systems Watanabe et al. 2021. For example, the simplest bead-spring model accounting for FENE effect, i.e., the FENE-PM-Rouse model, does not obey Cox-Merz rule, which was demonstrated to be valid for unentangled melts Colby et al. 2007. The difference between nonlinear flow behavior observed for entangled melts and solutions is also expected to hold for unentangled systems. In particular, friction reduction is expected to play a minor role in unentangled solutions of long chains in oligomers. The effect should be even more pronounced with respect to entangled solutions as, in unentangled regime, a long chain is almost entirely surrounded by oligomer, thus topological effects of other long chains are reduced. We note that monomeric friction reduction effects are more relevant for polystyrene due to the relatively low number of Kuhn steps between entanglements Anwar and Graham 2019. From an experimental point of view, unentangled solutions have a lower elasticity, i.e., lower characteristic elastic modulus compared to entangled ones, hence start-up experiments could be carried out at larger Weissenberg numbers, without artifacts induced by edge fracture.

Concerning the nonlinear flow behavior of H-polymer melts, an interesting aspect is the analogy with the linear counterpart. Ianniruberto and Marrucci argued that arm withdrawal in strong extensional flows makes the behavior of H-polymers similar to that of linear polymers with comparable span molecular weight Ianniruberto and Marrucci 2013. Furthermore, Baig and Mavrantzas demonstrated the similarity of shear thinning behavior between an unentangled H-polymer and a linear polymer with the same span chain length Baig and Mavrantzas 2010.

Experimental studies validating the conjectures discussed above are currently lacking. The aim of this paper is to contribute to fill in this gap by focusing on nonlinear shear rheological properties of H-polymer melts and solutions in the poorly entangled state. In particular, we consider a nearly unentangled H-polymer melt and two solutions made by diluting large molecular weight H-polymers in a linear

oligomer. As mentioned above, drawing an analogy between unentangled melts and solutions is challenging for several reasons. For example, it is still unclear which coarse-graining length could provide a unified picture of melt and solution dynamics. In order to keep our analysis as simple as possible, and provided that the H-polymer considered here features an entanglement plateau, we dilute the large molecular weight H-polymers in a way to match the same *nominal Z* of the corresponding melt, considering an entanglement molecular weight of the solution equal to $M_e(\varphi_H) = M_e(1)\varphi_H^{-\alpha}$, where $M_e(1)$ is the entanglement molecular weight of the melt, φ_H the volume fraction of H-polymer in solution, and α is the dilution exponent, assumed equal to unity. This oversimplified approach neglects dilution effects on the H-polymer dynamics. However, it allows to attain weakly or unentangled H-polymer solutions, as demonstrated from the respective viscoelastic spectra, and ensures a reasonable match between the scaled linear viscoelasticity of the H-polymer melt and one of the two solutions, which serves as a basis for the analysis of the nonlinear flow behavior. Nonlinear transient shear experiments are performed with cone-and-partitioned-plate fixtures to avoid artifacts induced by edge fracture Costanzo et al. 2018. Inspired by the work of Ianniruberto and Marrucci (2013) and by that of Baig and Mavrantzas (2010), we compare the behavior of the marginally entangled H-polymer melt with that of a linear counterpart having the same zero shear viscosity and a comparable span molecular weight. In spite of the different architecture, the analogy between the nonlinear shear behavior of the two systems is confirmed. Concerning the solutions, we demonstrate that the minor role of friction reduction coupled with FENE behavior dominates the nonlinear response inducing shear strain hardening and progressive failure of the Cox-Merz rule.

Materials and methods

The H-polymers used in this work were prepared by Roovers in 1981 Roovers and Toporowski 1981. In order to exclude possible degradation, we performed linear shear rheological measurements on the melts and compared our data with those of Roovers (1984). The difference between the current linear data and those digitized from reference Roovers (1984) was found lower than 10%. The linear polystyrene oligomer was purchased by Sigma Aldrich (USA) and has a $M_w = 1840$ Da and PDI=1.05. The linear polystyrene coded as PS71k was purchased from Polymer Source (Canada). It has $M_w = 71$ kDa and PDI=1.04.

In order to prepare the solutions of H-polymer in polystyrene oligomer, proper amounts of H-polymer and linear oligomer were dissolved in toluene in a glass vial. The vial was sealed with a cap and the mixture was put on gentle

stirring with a magnet at room temperature. After 24 h, the cap was removed and substituted with an aluminum foil with holes to allow for slow evaporation of toluene. After one week the residual amount of toluene was removed by putting the open vial in a vacuum oven for 48 h at room temperature. After this time, the temperature was increased to 160 °C for 2 h. Such a protocol ensured a residual amount of toluene smaller than 0.1% in the solutions. The polymer melts and prepared solutions are listed in Table 1. We used the same codes as in reference Roovers and Toporowski (1981). The two solutions were prepared by diluting H3A1A and H5A1 in linear oligomer at such a concentration to have the same nominal number of entanglements of the H-polymer H4A1A, according to the relation $Z(\varphi_H) = Z(1)\varphi_H^\alpha$, where $Z(\varphi_H)$ is the number of entanglements in solution and $Z(1)$ is the number of entanglements in the melt.

The glass transition temperatures were either taken from literature or measured through differential scanning calorimetry (DSC). To this end, a DSC Q2500 from TA instruments was used. Measurements were performed from 25°C to 180°C at a heating/cooling rate of 5°C/min in nitrogen atmosphere.

To perform rheological measurements, melts and solutions were shaped to discoid specimens by means of a homemade vacuum compression mold. Details of the design can be found in reference Costanzo et al. (2019). Linear and nonlinear rheological measurements were performed on two different rheometers. In particular we used an ARES rheometer (TA Instruments, USA) equipped with a homemade cone-and-partitioned plate fixture Costanzo et al. 2018 and a convection oven for temperature control. The homemade cone-and-partitioned plate has an inner plate with a 6 mm diameter. The cone has a diameter of 25 mm, a truncation of 104 μm and an angle of 6°. We also run measurements on a MCR702 rheometer (Anton Paar, Germany) equipped with a 8 mm commercial cone-and-partitioned plate fixture and a hybrid thermal control unit (CTD450). The cone used on the MCR702 has a

truncation of 50 μm and an angle of 4°. Nitrogen atmosphere was used in both cases to prevent degradation.

Results and discussion

Linear viscoelasticity

As mentioned above, the polymer volume fraction of the solutions was chosen in a way to match the same nominal number of entanglements of the melt H4A1A, based on the relation $Z(\varphi_H) = Z(1)\varphi_H^\alpha$. The dilution exponent was chosen to be equal to unity, although values between 1 and 4/3 were reported in literature. The uncertainty on the value of the dilution exponent affects $Z(\varphi_H)$ and the relaxation function $\mu(t) \propto \phi(t)^\alpha$ (see Appendix A). However, it has only a minor qualitative effect on the nonlinear rheological data and does not change the main outcome of nonlinear shear experiments, i.e., the failure of the Cox-Merz rule for solutions.

Figure 1a depicts the linear rheological properties of the H-polymer melts and the two solutions compared at the same distance from the glass transition temperature ($T_{ref} = T_g + 27$°C). The linear viscoelastic spectrum of the oligomer is also reported for completeness.

Regarding the high molecular weight melts, the low-frequency crossover could be barely detected for the sample H3A1A and was not observed for the sample H5A1 in the investigated temperature range. Note that frequency sweep tests were performed only up to 230°C. We did not include data at higher temperatures as evident degradation occurs in the experimental time window.

Both the arms and the backbone of H3A1A and H5A1 melts are entangled (see Table 1). Their relaxation spectrum can be rationalized based on the concepts of hierarchical relaxation McLeish 1988a, b and dynamic tube dilation Marrucci 1985; Kapnistos et al. 2005; Watanabe 2008; Lentzakis et al. 2019. The two melts exhibit a well-defined elastic

Table 1 Material properties of H-polymer melts and solutions investigated in this work. M_{w_b} is the backbone molecular weight; M_{w_a} is the molecular weight of a single arm. Z_b and Z_a are the number of entanglements per backbone and arm, respectively. T_g is the glass transition temperature and τ_d is the terminal relaxation time

Sample	φ_H [v/v]	M_{w_b} [Da]	M_{w_a} [Da]	Z_b	Z_a	T_g [°C]	τ_d [s]
H4A1A	1	1.90×10^4	1.90×10^4	1.1	1.1	98.5[a]	1.8[c]
H3A1A	1	1.23×10^5	1.23×10^5	7.2	7.8	100[a]	
H5A1	1	2.04×10^5	2.05×10^5	12.0	12.0	100[a]	
O2	1	1.84×10^3				60.0	
Lin PS71k	1	71.00×10^3				100[b]	2.3[c]
H3A1A-O2	0.146			1.1	1.1	63.2	127.8[d]
H5A1-O2	0.094			1.1	1.1	63.6	20.4[d]

[a]from reference Roovers (1984)

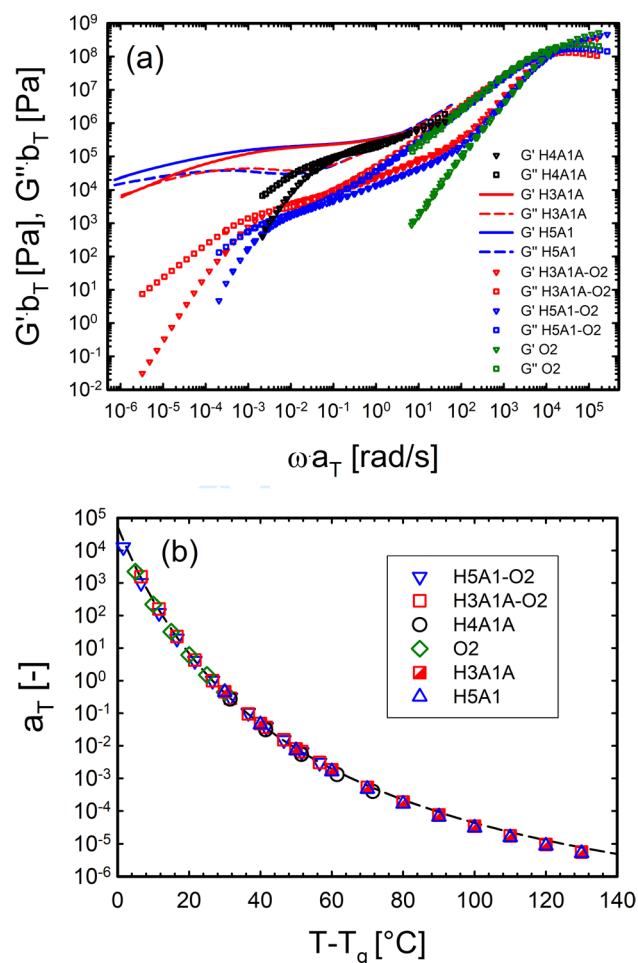[b]from reference Fox and Flory (1954)

[c]at 140°C

[d]at 150°C

Fig. 1 (**a**) Linear viscoelastic spectra and (**b**) shift factors of the H-polymer melts and solutions compared at a reference temperature equal to $T = T_g + 27°C$

regime, there is a strong cooperativity between the relaxation of arms and backbone of an H-shaped polymer, as discussed in reference Karayiannis and Mavrantzas (2005). In such a case, the relaxation of the H-polymer becomes akin to that of a linear polymer with comparable span molecular weight. If we consider a linear architecture with comparable molecular weight, the few entanglements of such polymer are enough to show a weak elastic plateau in the intermediate frequency range, as reported below.

Concerning the two solutions, the relaxation of the oligomeric matrix is much faster compared to the large H-polymer molecules, hence we can safely assume that the oligomer acts as a real solvent. Given the low volume fraction of polymer in the solutions, H macromolecules only have few entanglements hence they do not experience any *tube* constraint Lentzakis et al. 2019. Thus, typical dynamics of nearly unentangled systems are expected for solutions. The viscoelastic spectra were measured from terminal relaxation to the glassy regime. Thermorheological complexity emerges in the glass-to-rubber part of the relaxation spectrum (see Appendix B). In the high frequency range, the curves of both solutions virtually overlap the master curves of the oligomer, indicating that relaxation at short times concerns length scales comparable with the oligomeric one. The intermediate frequency range is dominated by the branches and backbone relaxation of the diluted H-polymer. For the solution H3A1A-O2, the polymer concentration is such that an elastic plateau typical of a weakly entangled system can still be observed. Conversely, the solution H5A1-O2 features a relaxation spectrum typical of unentangled systems, conforming to a Rouse-like power law relaxation before terminal flow is approached. Analogous behavior was found for a solution of H3A1A in polystyrene oligomer with $M_w = 5$ kDa at $\phi = 10\%$ Lentzakis et al. 2019. In the latter case, the data were modelled by using a Rouse spectrum with no retardation factor arising from branching points, due to the almost unentangled environment.

Figure 1b depicts the horizontal shift factors used to build the master curves of Fig. 1a. Vertical shift was found negligible. When reported at the same distance from the glass transition temperature, the data collapse onto a single master curve, confirming that the samples are compared at isofrictional state. The values of the WLF fit constants of the different samples at the same distance from T_g are very similar. For clarity, a single WLF fit line of the data is reported in Fig. 1b (dashed line). The WLF constants of such curve are obtained as the arithmetic average of the WLF constants of the single samples. The values are $c_1 = 8.89 \pm 0.56$ and $c_2 = 76.46 \pm 3.48$ °C.

As mentioned above, several authors pointed out similar dynamics between linear and H-polymers in strong nonlinear flows Ianniruberto and Marrucci 2013; Baig and Mavrantzas 2010. The analogy stems from the assumption that, at high

plateau in the intermediate frequency range which can be attributed to the entanglement network of the branches. After the branches have relaxed by arm retraction, the backbone relaxes at first by fluctuation modes of the segments and eventually by reptation Lentzakis et al. 2019. The branching points have two competing effects on the backbone relaxation van Ruymbeke et al. 2006. The backbone experiences extra friction due to the slow diffusion of the branching points. However, the relaxed branches act as a solvent for backbone relaxation, speeding up the dynamics.

The sample H4A1A is only marginally entangled as it only has one entanglement per arm and one per backbone. If the relaxation time scales of the arms and backbone were well separated both of them should relax via Rouse-like dynamics, therefore no elastic plateau should arise in the relaxation spectrum. However, a weak elastic plateau is observed experimentally for this sample (see Fig. 1). We attribute this feature to the fact that, in a weakly entangled

flow rates, the H-polymer coil strongly aligns in the flow direction, becoming similar to that of a linear polymer with chain length equal to the span length of the H-polymer. The span length is calculated based on the longest end-to-end path of the H-polymer, hence it is equal to the sum of the branch-backbone-branch length. Since, H4A1A is symmetric, the span molecular weight is equal to $M_s = 3 \times 1.9 = 57$ kDa. However, we decided to compare the rheology of H4A1A with that of a linear polystyrene with $M_w = 71$ kDa. Although this molecular weight is slightly larger than M_s, such linear polymer has approximately the same zero shear viscosity of H4A1A. Furthermore, since the two samples have the same chemistry and the same glass transition, they feature the same glass relaxation and entanglement plateau. This ensures a fair comparison in both linear and nonlinear regimes. Figure 2 compares the linear master curves of the two polymers at the same reference temperature ($T_{\text{ref}} = 140$ °C). The zero shear viscosity of PS71k agrees well with the expected value reported in literature Casale et al. 1971. The two samples have virtually the same zero shear viscosity. Moreover, the complex viscosity agrees well in both Newtonian and power law regimes. On the other hand, the branched architecture of the sample H4A1A results in a broader transition from the Newtonian plateau to the power law region, as expected.

Nonlinear start-up shear tests

Nonlinear start-up shear tests were performed on both the melt H4A1A and the solutions H3A1A-O2 and H5A1-O2. The results are reported in Fig. 3.

Gray colors represent data obtained at a higher temperature (115°C) and shifted by means of the shift factors of Fig. 1b. The blue lines are LVE envelopes obtained from the data of Fig. 1a. To calculate the LVE envelopes, the
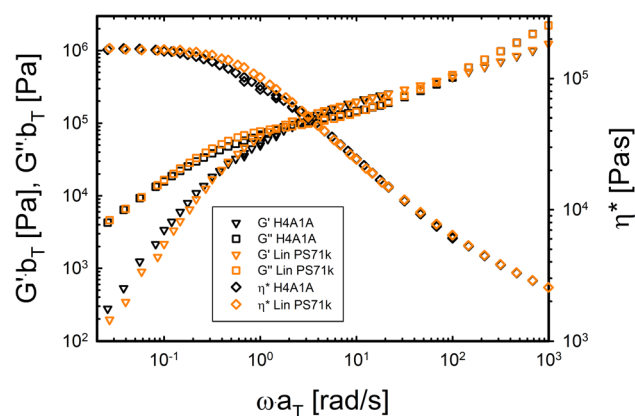
Fig. 3 Start-up shear tests performed on (**a**) H4A1A at T=140°C, (**b**) H3A1A-O2 at T=100°C, (**c**) H5A1-O2 at T=100°C. Shear rates in s^{-1} are reported in the legend. The data in gray color were measured at 115°C and shifted to 100°C by means of the shift factors of Fig. 1b

Fig. 2 Linear viscoelastic spectra of the H-polymer H4A1A and the linear monodisperse polystyrene Lin PS71k, compared at the same reference temperature $T_{\text{ref}} = 140$°C
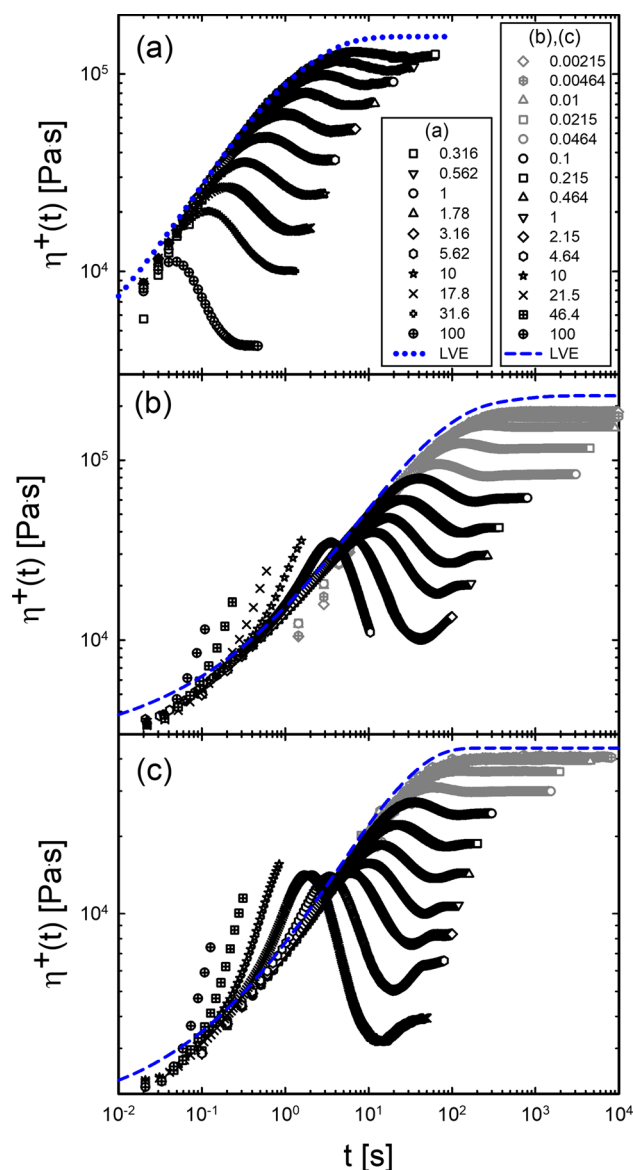
dynamic data were fitted with a discrete Maxwell relaxation spectrum of n modes, through the IRIS software (IRIS Development LLC, USA). Then, the viscosity was calculated as Schweizer and Schmidheiny 2013:

$$\eta(t) = \sum_{i=1}^{n} G_i \tau_i \left[1 - \exp\left(-\frac{t}{\tau_i} \right) \right] \tag{1}$$

where G_i and τ_i are the set of Maxwell moduli and relaxation times, respectively. The relaxation spectra of both melt and solutions are reported in (Appendix C).

Start-up viscosity data of solutions at high rates are cut before overshoot because axial transducer overload induced by strain hardening occurred.

The melt H4A1A is only weakly entangled. In the range of explored shear rates the sample undergoes strain softening behavior typical of polymer melts. Data on start-up shear tests of well-entangled H-polymer melts such as H3A1A were reported by Snijkers and Vlassopoulos (2014) and Snijkers et al. (2013). The transient nonlinear shear behavior displays analogies with that of other branched systems such as comb polymers Snijkers et al. 2013. The latter undergo a double stress overshoot before approaching steady state. The first overshoot is due to stretch of the side branches whereas the second overshoot is due to the stretch of the backbone, which occurs after the branches have been withdrawn into the backbone tube. Comb polymers generally have side branches much shorter than the backbone, hence, the time scales for branch and backbone stretch are well separated and the two stress overshoots can be clearly distinguished. In nearly symmetric entangled H-polymers, the difference in time scales for stretching backbone and branches is not as neat as for combs. Consequently, the double overshoot is less evident and a relatively broad overshoot is observed, instead. Such a feature was also reported for other branched systems such as stars Snijkers et al. 2013 and regular dendrimers Huang et al. 2017. On the other hand, since the melt H4A1A is only marginally entangled, the features described above are less evident.

The nonlinear start-up shear behavior of H4A1A was compared with that of the linear PS71k. Figure 4 reports the comparison between start-up shear data on the samples H4A1A and the linear PS71k at the same temperature (T=140°C).
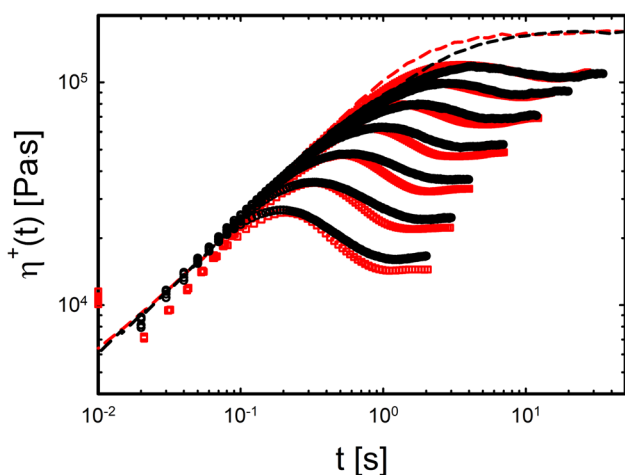
Since the glass transition temperature of the two polymers is the same, such a condition also corresponds to the same distance from T_g. In the available range of shear rates, the data overlap fairly well. The only difference between the data sets is observed in the broadness of the overshoot, which is slightly larger for the H-polymer. The validity of the analogy between linear and branched polymers in strong flows relies on the fact that molecular mechanisms such as branch withdrawal and alignment in the direction of flow reduce the branched architecture to a linear one Ianniruberto and Marrucci 2013. As a consequence, the shear thinning behavior of an H-polymer is close to that of a linear polymer of same span chain length, as demonstrated by means of molecular dynamics simulations for unentangled H-polymer melts Baig and Mavrantzas 2010.

Figure 5 reports the normalized Cox-Merz rule for the H-polymer melt and the two solutions.

The complex and steady shear viscosity values were divided by the zero shear viscosity, η_0. Both frequency and shear rate values were multiplied by the terminal relaxation time, τ_D, to obtain the Deborah (De) and Weissenberg (Wi_D) number, respectively. The terminal relaxation time for both melts and solutions is reported in Table 1. It was obtained from the low frequency limit of the product between the zero shear viscosity and the steady state recoverable compliance J_e, according to Eq. 2.

$$\tau_D = \eta_0 J_e = \lim_{\omega \to 0} \frac{G'(\omega)}{\omega G''(\omega)} \tag{2}$$

The linear polystyrene PS71k is also reported for comparison. Both the linear and H-polymer melts follow the Cox-Merz rule, as expected. It was found that linear entangled polymer melts
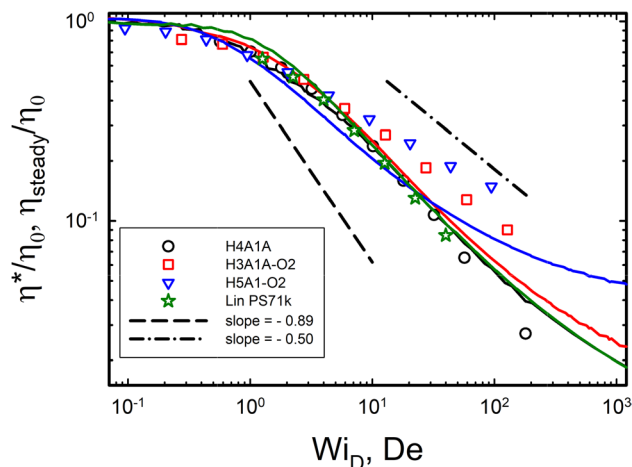

Fig. 4 Comparison of start-up shear data of H4A1A (black symbols) and PS71k (red symbols). Shear rates (from top to bottom, in s^{-1}) = (0.562, 1, 1.78, 3.16, 5.62, 10, 17.8). Dashed lines represent the LVE envelopes

Fig. 5 Normalized complex viscosity (solid lines) as a function of the Deborah number and normalized steady state viscosity (symbols) as a function of the Weissenberg number. Solid lines correspond to symbols with the same color. Dashed and dash-dotted lines indicate characteristic slopes, as reported in the legend

have a slope of -0.89 Parisi et al. 2021 whereas unentangled ones have a slope of -0.5 Colby et al. 2007. Since the PS71k is only marginally entangled, the thinning slope has an intermediate value. From best fit through the data, a value of -0.61 is found. The shear thinning behavior of H4A1A is the same as PS71k. Concerning the solutions, Cox-Merz is not verified. In particular, the thinning slope decreases upon dilution. For H3A1A-O2, a best fit through the data yields a thinning slope of -0.46 whereas for the H5A1-O2 a slope of -0.35 is found. The decreasing thinning slope indicates a flattening of the viscosity curve towards an asymptotic value as maximum stretch is approached. The difference between the nonlinear behavior of the melt and the solutions can be explained based on monomeric friction reduction. Dynamics of linear unentangled polymers have been described based on a FENE-Rouse model including monomeric friction reduction and variation of the Brownian force intensity Sato et al. 2021. The similarity between H and linear polymers in strong flows has been already highlighted above. Therefore, despite the different architecture, it is reasonable to retain a qualitatively similar picture for the behavior of H-polymers in nonlinear flows. At high shear rates, the H molecules of the melt strongly align in the flow direction. As a consequence, monomeric friction reduction occurs in such a direction, inducing the decrease of viscosity. On the other hand, friction reduction effects are minor for solutions as the fast relaxation of the oligomer creates an isotropic environment around the H-polymer. With a lesser effect of friction reduction, the FENE behaviour of the chain emerges, inducing transient shear strain hardening and a smaller viscosity thinning at high rates. As mentioned in the introduction, another possible explanation for the failure of Cox-Merz rule is the extra stress coming from backbone stretch which increases with dilution Snijkers and Vlassopoulos 2014.

The transient nonlinear behavior was further investigated by analyzing the viscosity overshoot. Figure 6a reports the strain value γ_{MAX} corresponding to the peak viscosity as a function of the Weissenberg number for both melts and solutions whereas Fig. 6b shows the peak broadness evaluated with the same procedure of reference Snijkers et al. (2013).

The stress overshoot appears as soon as nonlinear regime is approached, that is at $Wi_D \approx 1$. At low rates, it is associated with polymer coil orientation in the flow direction whereas at high rates it is the result of both orientation and stretch. At low rates γ_{MAX} is nearly constant with a value of 2.3, consistently with tube model predictions. At high rates, γ_{MAX} increases with increasing shear rate as a power law. The expected slope for entangled linear polymers is 0.33 Snijkers and Vlassopoulos 2011; Costanzo et al. 2016 and it is related to polymer stretch and recoil dynamics Xie and Schweizer 2018. Since the polymers examined here are in the marginally entangled regime, we observe that data related to H4A1A and PS71k have a slope of 0.2. Concerning the solutions, the slope of the power law increases upon dilution and reaches much
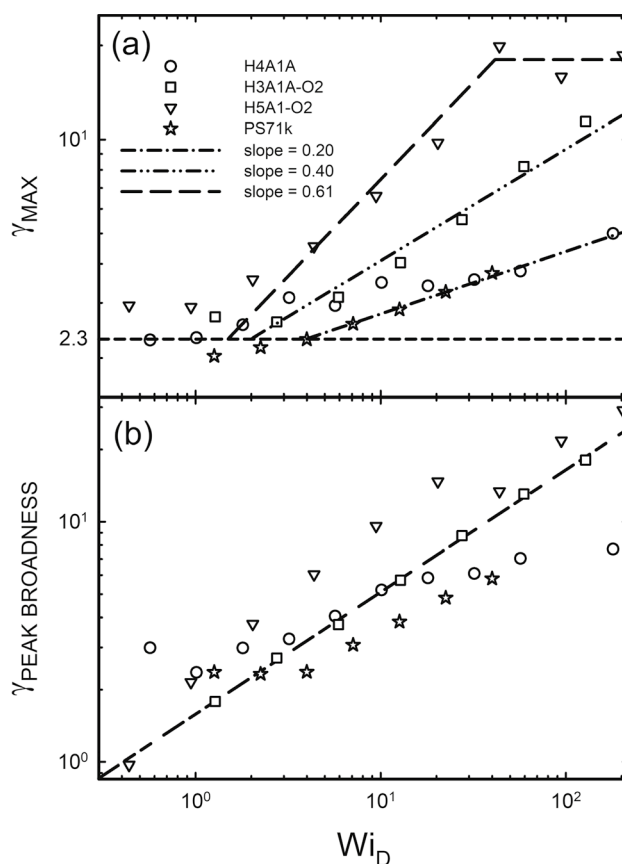

Fig. 6 (a) Strain corresponding to the maximum viscosity and (b) broadness of viscosity overshoot as functions of the Weissenberg number. Dashed lines indicate characteristic slopes, as reported in the legend. The slope of the dashed line in panel b is 0.5

larger values compared to melts in the same range of Weissenberg numbers. The lines are linear fits through the data. The increase of the slope can be attributed to the increased extensibility of the molecule upon dilution, that is, a larger stretch ratio $\lambda = \sqrt{N_k}$, where N_k is the number of Kuhn steps of a linear chain with the same span molecular weight of the H-polymer. At fixed Weissenberg number, a chain with larger extensibility requires a larger strain before critical stretch occurs determining the viscosity peak. We observe that, for the most dilute solution, the peak strain saturates at a value of approximately 20 strain units, indicating that the maximum stretch of the molecule is likely approached.

Concerning the data related to peak broadness (Fig. 6b), it seems that solutions exhibit a slightly wider overshoot compared to melts. However, due to the scattering of the data, it is difficult to draw conclusive remarks. On the other hand, it is interesting to observe that, by comparing Fig. 6a and b, at the same Weissenberg number, the solution featuring a larger maximum strain at viscosity peak also shows a broader overshoot. This suggests that the two parameters are related to elastic stretch and recoil dynamics, as already pointed out for entangled linear networks Xie and Schweizer 2018. In

general, the scaling of the data upon the Weissenberg number seems to obey a power law with an exponent of approximately 0.5 (best fit through the data), as reported in Fig. 6b.

Besides the peak strain and broadness, another parameter associated with the amount of molecular coil deformation is the ratio between the peak and steady state viscosity, η_{MAX}/η_{STEADY}. Furthermore, start-up shear data of polymer melts and solutions in strong flows feature an undershoot preceeding steady state. The undershoot is generally larger for solutions. Akin to overshoot, the viscosity undershoot can be analyzed by plotting the ratio between the undershoot and steady state viscosity, η_{MIN}/η_{STEADY}. Figure 7 reports both parameters as functions of the Weissenberg number for linear and H-polymer melts and solutions.

For entangled linear polymers in fast shear flows, it was observed that the ratio between the maximum and steady state viscosity increases upon the Weissenberg number as a power law. The exponent of such power law was approximately 0.25 Costanzo et al. 2016. For the weakly entangled H-polymer melts and solutions investigated here, as well as for PS71k, a best fit through the data yields an exponent of 0.2. However, the scattering of the data is too large to resolve a possible difference between the two regimes. For both linear and H-polymers, the value of the ratio deviates from unity when chain stretch occurs. In the same range of the explored Weissenberg numbers, H-polymer solutions exhibit a clear undershoot, in contrast to melts. The viscosity undershoot observed for the solutions showed an unambiguous dependence on the Weissenberg number, albeit small. Figure 7 reports the normalized undershoot as a function of Wi_D (data in gray). The data align on a power law trend with a slope of -0.05. We anticipate that such scaling is consistent with that observed for other polymeric solutions of different molecular architectures. We also note that the deviation from unity of
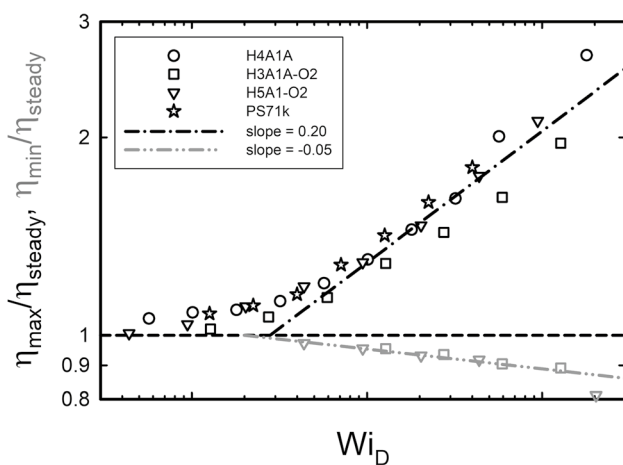

Fig. 7 Ratio of the overshoot to steady state viscosity, η_{MAX}/η_{STEADY} (black symbols), and ratio of the undershoot to steady state viscosity, η_{MIN}/η_{STEADY} (gray symbols), as functions of the Weissenberg number

the two parameters seems to occur at the same Weissenberg number. This suggests that undershoot could be related to recoil from stretch, as already speculated for comb polymers Snijkers et al. 2013. Recently, undershoot in linear polymers was also associated to molecular tumbling Costanzo et al. 2016. The data reported here do not allow for a conclusive explanation of the molecular mechanism of undershoot. Therefore, we limit our analysis to the scaling, remarking that neither elastic recoil nor tumbling are in contrast with nonlinear dynamics of nearly unentangled H-polymers.

Conclusions

We explored the linear and nonlinear shear rheology of nearly unentangled polystyrene H-polymer melts and solutions. The solutions were prepared diluting large molecular weight H-polymers in linear oligomeric solvent, at a volume fraction such as to attain a similar number of entanglements of the corresponding melt. This approach does not take into account dilution effects on H-polymer dynamics in nearly unentangled state. On the other hand, the data clearly indicate that dilution plays a role as, in spite of the similar topology, solutions relax faster than the corresponding melt. This also suggest that, possibly, a dilution exponent larger than unity should be considered for the comparison.

In spite of the different molecular architecture, the nonlinear rheological behavior of marginally entangled polymer melts shares common features with that of linear polymers with approximately the same span molecular weight. In particular, we compared the H-polymer melt with a linear polymer having same zero shear viscosity. We found that both H-shaped and linear polymer are shear thinning. They obey Cox-Merz rule with the same thinning exponent.

Conversely, transient strain hardening and failure of Cox-Merz rule are observed for solutions. In particular, the thinning exponent decreases upon dilution.

These observations are explained based on monomeric friction reduction, which occurs when chains are strongly aligned in the flow direction. Friction reduction is more relevant for melts, as a given chain is surrounded by other chains aligned in the same direction. Conversely, a given chain in solution is surrounded by oligomers, which relax on a much faster time-scale and keep a randomly oriented environment around the long chain. Subsequently, friction reduction plays a lesser role for solutions. This feature, coupled with the FENE behavior of unentangled systems, is at the origin of transient shear hardening. The rheological features observed in this study claim for a deeper understanding of the linear and nonlinear dynamics of branched architectures. It is hoped that this work will encourage further studies on the behavior of melts and solutions of complex architectures in the marginally entangled or unentangled state.

Appendix A. Comparison between H-polymer melts and solutions

Entangled linear polymer melts and solutions with the same number of entanglements have same linear scaled viscoelastic properties Costanzo et al. 2016. Here, we attempt at drawing a similar analogy for the H-polymer melt and the solution H3A1A-O2, for which a weak elastic plateau could still be detected. In Fig. 8, the scaled viscoelastic master curves of the H4A1A melt and the H3A1A-O2 solution are compared.

The viscoelastic master curves of the melt and the solution were scaled by dividing both loss and storage moduli by the plateau value of the elastic modulus, G_N^0 evaluated at the minimum of the loss factor, $\tan(\delta)$. The frequency axis was multiplied by the entanglement time, τ_e, obtained as the inverse of the high frequency crossover of the viscoelastic moduli. The scaled master curves overlap well in the high frequency part. However, it is evident that the relaxation of the solution is faster compared to that of the melt. Hence, in spite of similar topology, dilution by oligomer speeds up the dynamics. Such trend is confirmed by the fact that the most dilute solution, H5A1-O2, features no elastic plateau. This also suggests that the effective number of entanglements in solutions might be lower than the nominal one, that is, the dilution exponent might be larger than unity. A systematic analysis of the scaled rheological properties of melts and solutions represents a good strategy to quantify dilution effects. However, this is beyond the scope of the present work. As mentioned above, dynamic dilution effects have larger consequences on the solution prepared with the largest molecular weight H-polymer, H5A1-O2, where unentangled scaling is observed (see Fig. 1a).
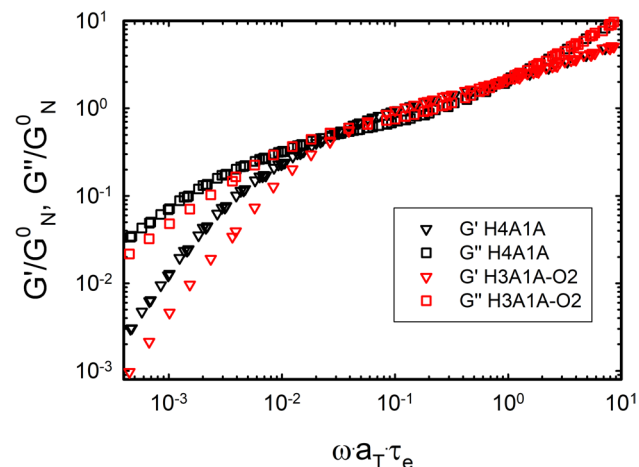
Appendix B. Thermorheological complexity of H-polymer solutions

A remark is in order about the thermorheological complexity observed for the two solutions in the glass-to-rubber part of the relaxation spectrum. Several authors have pointed out that a thermorheologically complex behavior is observed in this zone for many polymer species, including polystyrene Plazek 1965; Inoue et al. 1991, 1996 . The reason is that the relaxation spectrum features two components at the transition, one related to the elastic plateau region and the long-time relaxation of the glass, and another related to the properties of the glassy zone. Such components have different temperature dependencies Osaki et al. 1995. Therefore, time-temperature superposition (TTS) works only apparently in this region. The failure of TTS cannot be appreciated on the scale of Fig. 1a. To highlight this aspect, Van Gurp-Palmen plots of the dynamic data of the two solutions were made Van Gurp and Palmen 1998 (Fig. 9). It is clear that, for both solutions, the dynamic data do not overlap around the maximum of the phase angle, indicating thermorheological complexity. From the x-axis, it can be observed that
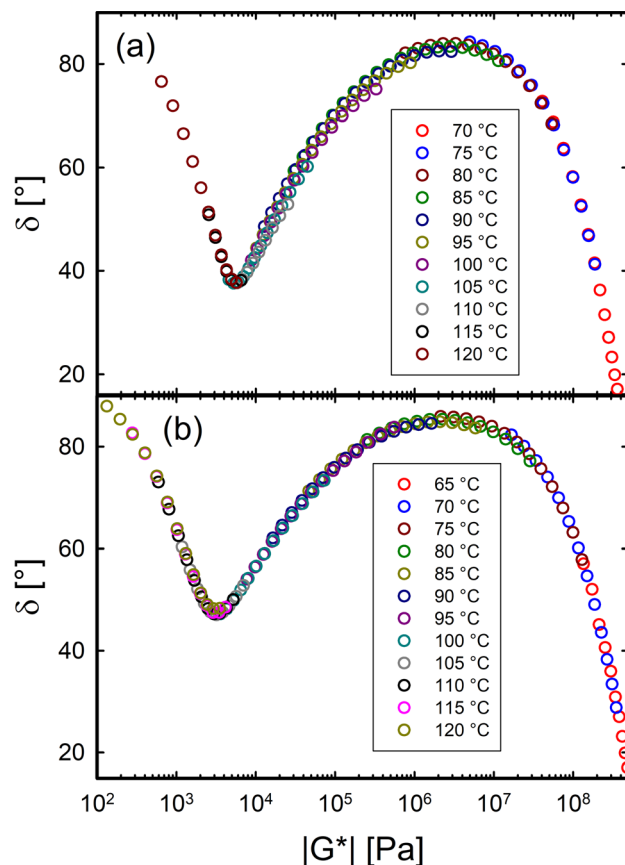

Fig. 8 Comparison of the scaled linear viscoelastic spectra of the polymer melt H4A1A and the polymer solution H3A1A-O2

Fig. 9 Van Gurp-Palmen plots of (**a**) H3A1A-O2 and (**b**) H5A1-O2 solutions

the values of the complex modulus at which TTS correspond to the rubbery-to-glassy transition region of the master curves.

Appendix C. LVE discrete spectra of the melts and solutions

In table 2, the discrete relaxation spectra of the H-polymer melt H4A1A and the two solutions H3A1A-O2 and H5A1-O2 are reported. The dynamic data of the two solutions were collected from the glass to the terminal relaxation, hence a larger number n of Maxwell modes is needed to properly fit the data in the whole frequency range.

Table 2 Discrete relaxation spectra of the melt H4A1A and the solutions H3A1A-O2 and H5A1-O2 calculated through the IRIS software

H4A1A		H3A1A-O2		H5A1-O2	
G_i [Pa]	τ_i [s]	G_i [Pa]	τ_i [s]	G_i [Pa]	τ_i [s]
1.10E+07	2.02E-04	1.38E+08	6.17E-07	2.01E+08	2.89E-07
4.53E+05	3.64E-03	1.40E+08	2.91E-06	1.94E+08	1.44E-06
1.66E+05	2.15E-02	1.10E+08	1.02E-05	1.30E+08	5.07E-06
1.05E+05	1.13E-01	2.57E+07	3.57E-05	3.09E+07	1.59E-05
9.68E+04	3.89E-01	1.70E+06	1.77E-04	3.51E+06	5.90E-05
3.79E+04	1.89E+00	2.10E+05	1.28E-03	3.12E+05	3.33E-04
5.56E+03	4.74E+00	5.40E+04	8.50E-03	6.45E+04	2.31E-03
		2.35E+04	3.39E-02	2.22E+04	1.76E-02
		1.04E+04	1.45E-01	8.74E+03	1.16E-01
		5.72E+03	6.29E-01	3.30E+03	7.99E-01
		2.88E+03	3.25E+00	1.66E+03	5.81E+00
		2.59E+03	1.89E+01	9.69E+02	2.94E+01
		1.52E+03	8.26E+01		
		6.81E+01	5.12E+02		

References

Anwar M, Graham RS (2019) Nonlinear shear of entangled polymers from nonequilibrium molecular dynamics. Journal of Polymer Science Part B: Polymer Physics 57(24):1692–1704. https://doi.org/10.1002/polb.24904

Baig C, Mavrantzas VG (2010) Tension thickening, molecular shape, and flow birefringence of an h-shaped polymer melt in steady shear and planar extension. The Journal of Chemical Physics 132(1):014904. https://doi.org/10.1063/1.3271831

Casale A, Porter RS, Johnson JF (1971) Dependence of flow properties of polystyrene on molecular weight, temperature, and shear. Journal of Macromolecular Science, Part C 5(2):387–408. https://doi.org/10.1080/15583727108085371

Colby RH, Boris DC, Krause WE, Dou S (2007) Shear thinning of unentangled flexible polymer liquids. Rheologica Acta 46(5):569–575. https://doi.org/10.1007/s00397-006-0142-y

Costanzo S, Huang Q, Ianniruberto G, Marrucci G, Hassager O, Vlassopoulos D (2016) Shear and extensional rheology of polystyrene melts and solutions with the same number of entanglements. Macromolecules 49(10):3925–3935. https://doi.org/10.1021/acs.macromol.6b00409

Costanzo S, Scherz LF, Schweizer T, Kröger M, Floudas G, Schlüter AD, Vlassopoulos D (2016) Rheology and packing of dendronized polymers. Macromolecules 49(18):7054–7068. https://doi.org/10.1021/acs.macromol.6b01311

Costanzo S, Ianniruberto G, Marrucci G, Vlassopoulos D (2018) Measuring and assessing first and second normal stress differences of polymeric fluids with a modular cone-partitioned plate geometry. Rheologica Acta 57:363–376. https://doi.org/10.1007/s00397-018-1080-1

Costanzo S, Pasquino R, Läuger J, Grizzuti N (2019) Milligram size rheology of molten polymers. Fluids 4(1), https://doi.org/10.3390/fluids4010028, https://www.mdpi.com/2311-5521/4/1/28

Cox WP, Merz EH (1958) Correlation of dynamic and steady flow viscosities. Journal of Polymer Science 28(118):619–622. https://doi.org/10.1002/pol.1958.1202811812

Das C, Inkson NJ, Read DJ, Kelmanson MA, McLeish TCB (2006) Computational linear rheology of general branch-on-branch polymers. Journal of Rheology 50(2):207–234. https://doi.org/10.1122/1.2167487

Doi M, Edwards SF (1978a) Dynamics of concentrated polymer systems. part 1.—brownian motion in the equilibrium state. J Chem Soc, Faraday Trans 2 74:1789–1801. https://doi.org/10.1039/F29787401789

Doi M, Edwards SF (1978b) Dynamics of concentrated polymer systems. part 2.—molecular motion under flow. J Chem Soc, Faraday Trans 2 74:1802–1817. https://doi.org/10.1039/F29787401802

Doi M, Edwards SF (1978c) Dynamics of concentrated polymer systems. part 3.—the constitutive equation. J Chem Soc, Faraday Trans 2 74:1818–1832, https://doi.org/10.1039/F29787401818

Doi M, Edwards SF (1979) Dynamics of concentrated polymer systems. part 4.—rheological properties. J Chem Soc, Faraday Trans 2 75:38–54, https://doi.org/10.1039/F29797500038

Doi M, Kuzuu NY (1980) Rheology of star polymers in concentrated solutions and melts. Journal of Polymer Science: Polymer Letters Edition 18(12):775–780. https://doi.org/10.1002/pol.1980.130181205

Dubbeldam JLA, Molenaar J (2009) Stress relaxation of star-shaped molecules in a polymer melt. Macromolecules 42(17):6784–6790. https://doi.org/10.1021/ma900863e

Fox TG, Flory PJ (1954) The glass temperature and related properties of polystyrene. Influence of molecular weight. Journal of Polymer Science 14(75):315–319. https://doi.org/10.1002/pol.1954.120147514

de Gennes PG (1971) Reptation of a polymer chain in the presence of fixed obstacles. The Journal of Chemical Physics 55(2):572–579. https://doi.org/10.1063/1.1675789

Graham RS, Likhtman AE, McLeish TCB, Milner ST (2003) Microscopic theory of linear, entangled polymer chains under rapid deformation including chain stretch and convective constraint release. Journal of Rheology 47(5):1171–1200. https://doi.org/10.1122/1.1595099

Hatzikiriakos SG (2000) Long chain branching and polydispersity effects on the rheological properties of polyethylenes. Polymer Engineering & Science 40(11):2279–2287. https://doi.org/10.1002/pen.11360

Huang Q, Mednova O, Rasmussen HK, Alvarez NJ, Skov AL, Almdal K, Hassager O (2013) Concentrated polymer solutions are different from melts: Role of entanglement molecular weight. Macromolecules 46(12):5026–5035. https://doi.org/10.1021/ma4008434

Huang Q, Hengeller L, Alvarez NJ, Hassager O (2015) Bridging the gap between polymer melts and solutions in extensional rheology. Macromolecules 48(12):4158–4163. https://doi.org/10.1021/acs.macromol.5b00849

Huang Q, Costanzo S, Das C, Vlassopoulos D (2017) Stress growth and relaxation of dendritically branched macromolecules in shear and uniaxial extension. Journal of Rheology 61(1):35–47. https://doi.org/10.1122/1.4966040

Ianniruberto G, Marrucci G (2013) Entangled melts of branched ps behave like linear ps in the steady state of fast elongational flows. Macromolecules 46(1):267–275. https://doi.org/10.1021/ma302131b

Ianniruberto G, Brasiello A, Marrucci G (2012) Simulations of fast shear flows of ps oligomers confirm monomeric friction reduction in fast elongational flows of monodisperse ps melts as indicated by rheooptical data. Macromolecules 45(19):8058–8066. https://doi.org/10.1021/ma301368d

Inoue T, Okamoto H, Osaki K (1991) Birefringence of amorphous polymers. 1. dynamic measurement on polystyrene. Macromolecules 24(20):5670–5675. https://doi.org/10.1021/ma00020a029

Inoue T, Mizukami Y, Okamoto H, Matsui H, Watanabe H, Kanaya T, Osaki K (1996) Dynamic birefringence of vinyl polymers. Macromolecules 29(19):6240–6245. https://doi.org/10.1021/ma960190r

Kapnistos M, Vlassopoulos D, Roovers J, Leal LG (2005) Linear rheology of architecturally complex macromolecules: Comb polymers with linear backbones. Macromolecules 38(18):7852–7862. https://doi.org/10.1021/ma050644x

Karayiannis NC, Mavrantzas VG (2005) Hierarchical modeling of the dynamics of polymers with a nonlinear molecular architecture: Calculation of branch point friction and chain reptation time of h-shaped polyethylene melts from long molecular dynamics simulations. Macromolecules 38(20):8583–8596. https://doi.org/10.1021/ma050989f

Lentzakis H, Costanzo S, Vlassopoulos D, Colby RH, Read DJ, Lee H, Chang T, van Ruymbeke E (2019) Constraint release mechanisms for h-polymers moving in linear matrices of varying molar masses. Macromolecules 52(8):3010–3028. https://doi.org/10.1021/acs.macromol.9b00251

Likhtman AE, Milner ST, McLeish TCB (2000) Microscopic theory for the fast flow of polymer melts. Phys Rev Lett 85:4550–4553. https://doi.org/10.1103/PhysRevLett.85.4550

Marrucci G (1985) Relaxation by reptation and tube enlargement: A model for polydisperse polymers. Journal of Polymer Science: Polymer Physics Edition 23(1):159–177. https://doi.org/10.1002/pol.1985.180230115

Matsumiya Y, Watanabe H (2021) Non-universal features in uniaxially extensional rheology of linear polymer melts and concentrated solutions: A review. Progress in Polymer Science 112:101325. https://doi.org/10.1016/j.progpolymsci.2020.101325

Matsumiya Y, Kumazawa K, Nagao M, Urakawa O, Watanabe H (2013) Dielectric relaxation of monodisperse linear polyisoprene: Contribution of constraint release. Macromolecules 46(15):6067–6080. https://doi.org/10.1021/ma400606n

Matsumiya Y, Masubuchi Y, Inoue T, Urakawa O, Liu CY, van Ruymbeke E, Watanabe H (2014) Dielectric and viscoelastic behavior of star-branched polyisoprene: Two coarse-grained length scales in dynamic tube dilation. Macromolecules 47(21):7637–7652. https://doi.org/10.1021/ma501561y

Matsumiya Y, Watanabe H, Masubuchi Y, Huang Q, Hassager O (2018) Nonlinear elongational rheology of unentangled polystyrene and poly(p-tert-butylstyrene) melts. Macromolecules 51(23):9710–9729. https://doi.org/10.1021/acs.macromol.8b01954

McLeish TCB (1988) Hierarchical relaxation in tube models of branched polymers. Europhysics Letters (EPL) 6(6):511–516. https://doi.org/10.1209/0295-5075/6/6/007

McLeish TCB (1988) Molecular rheology of h-polymers. Macromolecules 21(4):1062–1070. https://doi.org/10.1021/ma00182a037

McLeish TCB, Allgaier J, Bick DK, Bishko G, Biswas P, Blackwell R, Blottière B, Clarke N, Gibbs B, Groves DJ, Hakiki A, Heenan RK, Johnson JM, Kant R, Read DJ, Young RN (1999) Dynamics of entangled h-polymers: Theory, rheology, and neutron-scattering. Macromolecules 32(20):6734–6758. https://doi.org/10.1021/ma990323j

Milner ST, McLeish TCB, Likhtman AE (2001) Microscopic theory of convective constraint release. Journal of Rheology 45(2):539–563. https://doi.org/10.1122/1.1349122

Morelly SL, Alvarez NJ (2020) Characterizing long-chain branching in commercial hdpe samples via linear viscoelasticity and extensional rheology. Rheologica Acta 59(11):797–807. https://doi.org/10.1007/s00397-020-01233-5

Narimissa E, Rolón-Garrido VH, Wagner MH (2016) A hierarchical multi-mode msf model for long-chain branched polymer melts part ii: multiaxial extensional flows. Rheologica Acta 55(4):327–333. https://doi.org/10.1007/s00397-016-0922-y

Nielsen JK, Rasmussen HK, Denberg M, Almdal K, Hassager O (2006) Nonlinear branch-point dynamics of multiarm polystyrene. Macromolecules 39(25):8844–8853. 10.1021/ma061476r, URL https://doi.org/10.1021/ma061476r, https://doi.org/10.1021/ma061476r

Osaki K, Okamoto H, Inoue T, Hwang EJ (1995) Molecular interpretation of dynamic birefringence and viscoelasticity of amorphous polymers. Macromolecules 28(10):3625–3630. https://doi.org/10.1021/ma00114a016

Parisi D, Costanzo S, Jeong Y, Ahn J, Chang T, Vlassopoulos D, Halverson JD, Kremer K, Ge T, Rubinstein M, Grest GS, Srinin W, Grosberg AY (2021) Nonlinear shear rheology of entangled polymer rings. Macromolecules 54(6):2811–2827. https://doi.org/10.1021/acs.macromol.0c02839

Park SJ, Shanbhag S, Larson RG (2005) A hierarchical algorithm for predicting the linear viscoelastic properties of polymer melts with long-chain branching. Rheologica Acta 44(3):319–330. https://doi.org/10.1007/s00397-004-0415-2

Pearson DS, Helfand E (1984) Viscoelastic properties of star-shaped polymers. Macromolecules 17(4):888–895. https://doi.org/10.1021/ma00134a060

Plazek DJ (1965) Temperature dependence of the viscoelastic behavior of polystyrene. The Journal of physical chemistry 69(10):3480–3487

Roovers J (1984) Melt rheology of h-shaped polystyrenes. Macromolecules 17(6), 1996–1200

Roovers J, Toporowski PM (1981) Preparation and characterization of h-shaped polystyrene. Macromolecules 14(5):1174–1178. https://doi.org/10.1021/ma50006a007

van Ruymbeke E, Bailly C, Keunings R, Vlassopoulos D (2006) A general methodology to predict the linear rheology of branched polymers. Macromolecules 39(18):6248–6259. https://doi.org/10.1021/ma0604385

van Ruymbeke E, Kapnistos M, Vlassopoulos D, Huang T, Knauss DM (2007) Linear melt rheology of pom-pom polystyrenes with unentangled branches. Macromolecules 40(5):1713–1719. https://doi.org/10.1021/ma062487n

van Ruymbeke E, Muliawan EB, Hatzikiriakos SG, Watanabe T, Hirao A, Vlassopoulos D (2010) Viscoelasticity and extensional rheology of model cayley-tree polymers of different generations. Journal of Rheology 54(3):643–662. https://doi.org/10.1122/1.3368724

van Ruymbeke E, Shchetnikava V, Matsumiya Y, Watanabe H (2014) Dynamic dilution effect in binary blends of linear polymers with well-separated molecular weights. Macromolecules 47(21):7653–7665. https://doi.org/10.1021/ma501566w

Santangelo PG, Roland CM (2001) Interrupted shear flow of unentangled polystyrene melts. Journal of Rheology 45(2):583–594. https://doi.org/10.1122/1.1349711

Sato T, Kwon Y, Matsumiya Y, Watanabe H (2021) A constitutive equation for rouse model modified for variations of spring stiffness, bead friction, and brownian force intensity under flow. Physics of Fluids 33(6):063106. https://doi.org/10.1063/5.0055559

Scherz LF, Costanzo S, Huang Q, Schlüter AD, Vlassopoulos D (2017) Dendronized polymers with ureidopyrimidinone groups: An efficient strategy to tailor intermolecular interactions, rheology, and fracture. Macromolecules 50(13):5176–5187. https://doi.org/10.1021/acs.macromol.7b00747

Schweizer T, Schmidheiny W (2013) A cone-partitioned plate rheometer cell with three partitions (cpp3) to determine shear stress and both normal stress differences for small quantities of polymeric fluids. Journal of Rheology 57(3):841–856. https://doi.org/10.1122/1.4797458

Snijkers F, Vlassopoulos D (2014) Appraisal of the cox-merz rule for well-characterized entangled linear and branched polymers. Rheol Acta 53:935–946. https://doi.org/10.1007/s00397-014-0799-6

Snijkers F, Vlassopoulos D (2011) Cone-partitioned-plate geometry for the ares rheometer with temperature control. Journal of Rheology 55(6):1167–1186. https://doi.org/10.1122/1.3625559

Snijkers F, Ratkanthwar K, Vlassopoulos D, Hadjichristidis N (2013) Viscoelasticity, nonlinear shear start-up, and relaxation of entangled star polymers. Macromolecules 46(14):5702–5713. https://doi.org/10.1021/ma400662b

Snijkers F, Vlassopoulos D, Ianniruberto G, Marrucci G, Lee H, Yang J, Chang T (2013) Double stress overshoot in start-up of simple shear flow of entangled comb polymers. ACS Macro Letters 2(7):601–604. https://doi.org/10.1021/mz400236z

Snijkers F, Vlassopoulos D, Lee H, Yang J, Chang T, Driva P, Hadjichristidis N (2013) Start-up and relaxation of well-characterized comb polymers in simple shear. Journal of Rheology 57(4):1079–1100. https://doi.org/10.1122/1.4804198

Stadler FJ, Kaschta J, Münstedt H, Becker F, Buback M (2009) Influence of molar mass distribution and long-chain branching on strain hardening of low density polyethylene. Rheologica Acta 48(5):479–490. https://doi.org/10.1007/s00397-008-0334-8

Van Gurp M, Palmen J (1998) Time-temperature superposition for polymeric blends. Rheol Bull 67(1), 5–8

Wagner MH, Bastian H, Hachmann P, Meissner J, Kurzbeck S, Münstedt H, Langouche F (2000) The strain-hardening behaviour of linear and long-chain-branched polyolefin melts in extensional flows. Rheologica Acta 39(2):97–109. https://doi.org/10.1007/s003970050010

Watanabe H (2008) Dynamic Tube Dilation in Branched Polymers. Progress of Theoretical Physics Supplement 175:17–26. https://doi.org/10.1143/PTPS.175.17

Watanabe H, Ishida S, Matsumiya Y, Inoue T (2004) Viscoelastic and dielectric behavior of entangled blends of linear polyisoprenes having widely separated molecular weights: Test of tube dilation picture. Macromolecules 37(5):1937–1951. https://doi.org/10.1021/ma030443y

Watanabe H, Sawada T, Matsumiya Y (2006) Constraint release in star/star blends and partial tube dilation in monodisperse star systems. Macromolecules 39(7):2553–2561. https://doi.org/10.1021/ma0600198

Watanabe H, Matsumiya Y, van Ruymbeke E, Vlassopoulos D, Hadjichristidis N (2008) Viscoelastic and dielectric relaxation of a cayley-tree-type polyisoprene: Test of molecular picture of dynamic tube dilation. Macromolecules 41(16):6110–6124. https://doi.org/10.1021/ma800503e

Watanabe H, Matsumiya Y, Sato T (2021) Revisiting nonlinear flow behavior of rouse chain: Roles of fene, friction-reduction, and brownian force intensity variation. Macromolecules 54(8):3700–3715. https://doi.org/10.1021/acs.macromol.1c00013

Wingstrand SL, Alvarez NJ, Huang Q, Hassager O (2015) Linear and nonlinear universality in the rheology of polymer melts and solutions. Phys Rev Lett 115:078302. https://doi.org/10.1103/PhysRevLett.115.078302

Xie SJ, Schweizer KS (2018) Consequences of delayed chain retraction on the rheology and stretch dynamics of entangled polymer liquids under continuous nonlinear shear deformation. Macromolecules 51(11):4185–4200. https://doi.org/10.1021/acs.macromol.8b00671